

# We are IntechOpen, the world's leading publisher of Open Access books Built by scientists, for scientists

6,900

Open access books available

186,000

International authors and editors

200M

Downloads

Our authors are among the

154

Countries delivered to

TOP 1%

most cited scientists

12.2%

Contributors from top 500 universities



WEB OF SCIENCE™

Selection of our books indexed in the Book Citation Index  
in Web of Science™ Core Collection (BKCI)

Interested in publishing with us?  
Contact [book.department@intechopen.com](mailto:book.department@intechopen.com)

Numbers displayed above are based on latest data collected.  
For more information visit [www.intechopen.com](http://www.intechopen.com)



# Cone-Beam Computed Tomography in Dentomaxillofacial Radiology

*Bence Tamás Szabó, Adrienn Dobai and Csaba Dobo-Nagy*

## Abstract

The daily application of cone-beam computed tomography (CBCT) has been increasing. Not only the number of referrals has been raising, but also the variety of the anatomical regions requested for imaging is also growing in the dentomaxillofacial area. Even though computed tomography (CT) has been widely used in the head and neck region, by the invention of CBCT, some of the drawbacks of CT were overcome and turned into the advantages of the CBCT appliances, such as lower patient dose. In this chapter, we provide a comprehensive picture of the everyday use of CBCT as a modality in the dentomaxillofacial region and its current limitations and expected improvements.

**Keywords:** cone-beam computed tomography, dental digital radiography, diagnostic imaging, dentomaxillofacial radiology, incidental findings

## 1. Introduction

The use of cone-beam computed tomography (CBCT) has been increasing in everyday clinical practice. The advantages of CBCT contribute to its spreading not only in the field of dentistry, but also in maxillofacial surgery, otorhinolaryngology, rheumatology, and traumatology. Conventional-computed tomography (CT) has been widely used in the head and neck and other anatomical regions; nevertheless, by the invention of CBCT device for maxillofacial imaging in the 1990s [1], some of the drawbacks of CT were overcome resulting in the application of CBCT as an alternative modality in these regions. CBCT devices offer a compact size, the ability for producing high-resolution volumetric data, and lower patient dose compared to multislice CT (MSCT) [2–4]. Nonetheless, it should be noted that CBCT devices operate in a wide range of dose values [5]; hence, in the particular clinical situation, the proper justification and optimization are crucial. In this chapter, we provide a comprehensive picture of the everyday use of CBCT as a modality in the dentomaxillofacial region and its current limitations and expected improvements.

## 2. Basic principles of the CBCT

### 2.1 Image acquisition

The CBCT device consists of an X-ray source and a flat-panel detector, which are connected by a C-arm in a fixed position, but their vertical position can be

adjusted according to the anatomical circumstances of the patient. The X-ray source and the detector rotate in the opposite direction from  $180^\circ$  to  $360^\circ$  depending on the exposure setting of the device during the acquisition around the patient's head. The patient is in a standing, sitting, or supine position. In the latter case, the X-ray source and the detector are in a fixed position but rotate in the vertical plane. The average time of the exposure is varying from 5 to 40 s [6] depending on the device and the exposure settings. However, the energy of X-rays generated is usually diverse; hence, not only high but also low energy X-rays leave the X-ray source, which would be absorbed by the soft tissues and would not contribute to the imaging just to the increase of the patient dose. Therefore, low energy X-rays must be absorbed by an aluminum filter or a copper filter [7]. The divergent X-rays emitted from the X-ray tube are usually collimated by lead alloy with a rectangular opening, whose size can be adjusted depending on the size of the exposed volume, i.e., the field of view (FOV). Collimation results in the formation of a cone or pyramidal beam [8], as opposed to conventional CT devices where a fan beam leaves the collimator (**Figure 1**). However, today's MSCTs are using increasingly divergent beams due to the presence of detector rows [9].

During the acquisition, X-rays leave the tube either continuously or in pulse mode, in the latter allowing that the energy passes through the examined volume only at a particular rotation step leading to the reduction of radiation exposure suffered by the patient [7, 10, 11]. Numerous projection images are recorded on the detector during the rotation of the X-ray source and the detector. Unlike conventional CTs, where the patient table is constantly moving during the acquisition, each slice needs to be reconstructed separately to create the entire image data of the volume. The CBCT detector records the incoming X-rays, which were previously passed through and attenuated in various ways by the patient, and transforms them into an electrical signal, which is transmitted to the reconstruction computer. In case of flat-panel detectors (FPDs) such as the thin film transistor (TFT) containing amorphous silicon (a-Si) or

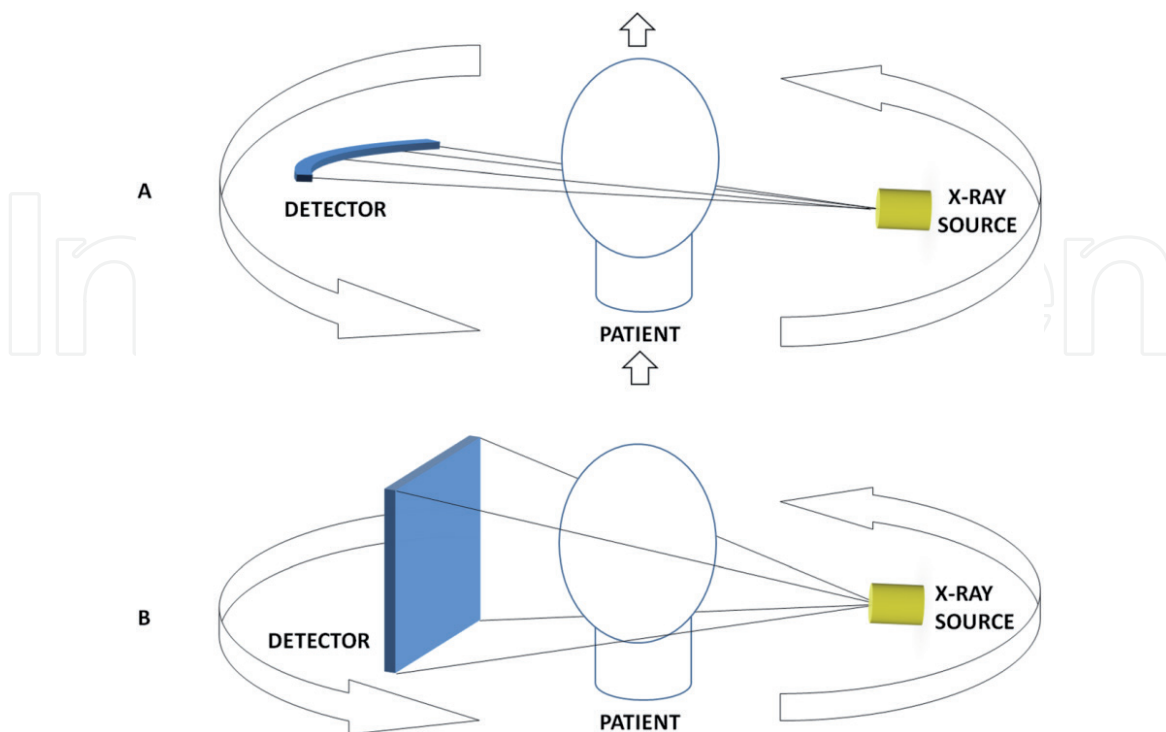


**Figure 1.** During the operation of a conventional CT device, the X-ray beam leaving the X-ray tube is fan-shaped and is detected by detector elements arranged in an arc rotating in a direction opposite to the X-ray source around the patient lying on the moving patient table (A). By contrast, CBCT applies a cone-shaped beam during image acquisition, which is recorded by a flat-panel detector (B).

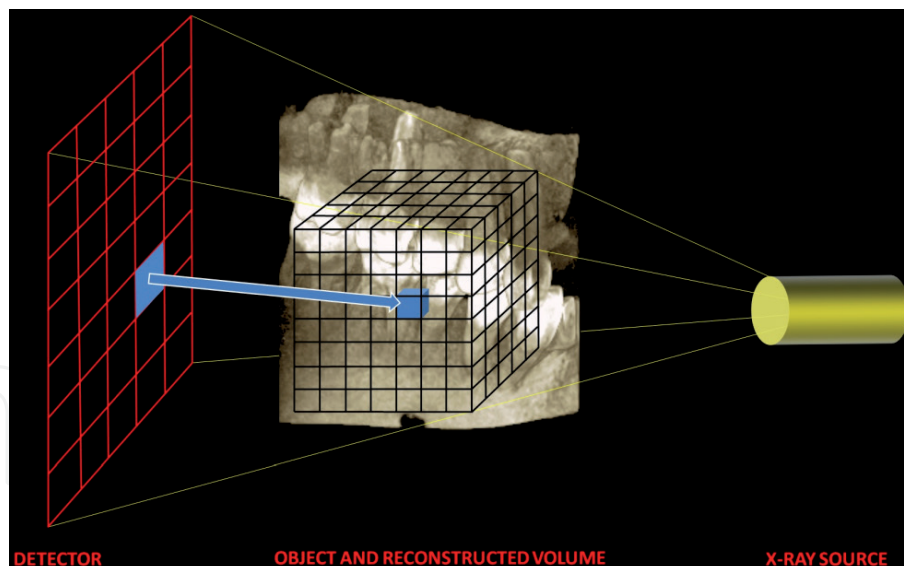


**Figure 2.**  
*The reconstruction algorithm projects back a gray value to a voxel according to a particular pixel of the detector on which the intensity of the attenuated X-ray beam was recorded.*

complementary metal oxide semiconductor (CMOS), the captured raw image dataset will be appeared as a cylindrical volume after the reconstruction in general [8, 12].

## 2.2 Image reconstruction

From raw images obtained during the CBCT acquisition, the computer in most cases uses the filtered back projection (FBP) algorithm for CBCT images: the Feldkamp-Davis-Kress (FDK) algorithm [13]. The reconstruction software assigns a grayscale value on a 12-bit scale, in some cases a 16-bit scale, depending on the degree of attenuation (usually the smallest grayscale value corresponds to the air) to each intensity value derived from the linear attenuation of the X-rays passing through the tissues on the pixel matrix of the detector [8]. The FDK algorithm projects back these values to each virtual component of the imaged, namely to each voxel (**Figure 2**). Subsequently, the reconstructed image will be displayed on the monitor as a real volumetric dataset.

## 3. Artifacts

One of the disadvantages of CBCT is the presence of artifacts that may significantly affect the image quality and interfere with the evaluation of the data [9]. Artifact can be defined as any lesion that is not physically present in the real structure of the imaged volume; nevertheless, it is detectable on the reconstructed image [9, 14]. One of the common artifacts is the beam hardening, which is generated by the polychromatic nature of the X-rays leaving the X-ray tube: the lower energies are absorbed in the tissues with higher absorption capacity; thus, the energy of the X-rays reaching the detector is proportionally higher than its energy emitted just from the X-ray tube. The artifact appears as alternating dark bands and stripes (**Figure 3**) or as a cupping pattern. The latter is explained by the fact that when a homogeneous cylindrical structure is imaged, the energy of the X-rays passing through the center of the volume is “hardened” at a greater level than at the periphery of the object. This leads to a saucer-like shape in the reconstructed image: transparency (i.e., lower grayscale values) in the center area of the scanned object, which decreases steadily as the periphery of the cylindrical structure [15].

Scatter leads to commonly the appearance of dark streaks similar to beam hardening, caused by the interaction between the X-ray and the material of the scanned object. In this case, the original direction of some X-ray photons changes causing computational error in the FDK algorithm. This leads to a decrease in contrast and distortion of grayscale values; however, by increasing the exposure energy and reducing the field of view, scatter can be reduced [7, 9]. It is important to note that selecting a smaller FOV can lead to the “local tomography” effect due to just a part of the object will be counted in the FDK algorithm as the scanned area and the surrounding tissues, which were out of the FOV, will disturb the computational process and the reconstructed image [14].

If a high atomic number material (e.g., metal) is in the path of the X-ray, the element of the detector only records very low intensity value and causes inconsistency during the FDK algorithm. This results in a dark, empty area, or radial streaking in the reconstructed image, which can impair the analysis of the image even on slices further away [9, 16] (**Figure 4**). In English literature, this phenomenon is known as extinction, “missing value,” or metal artifacts [8, 14, 15].

The position of the patient during the acquisition has a significant impact on the quality of the reconstructed image data. The FDK algorithm assumes motion-free, constant geometry [9]; therefore, during image acquisition, the changes

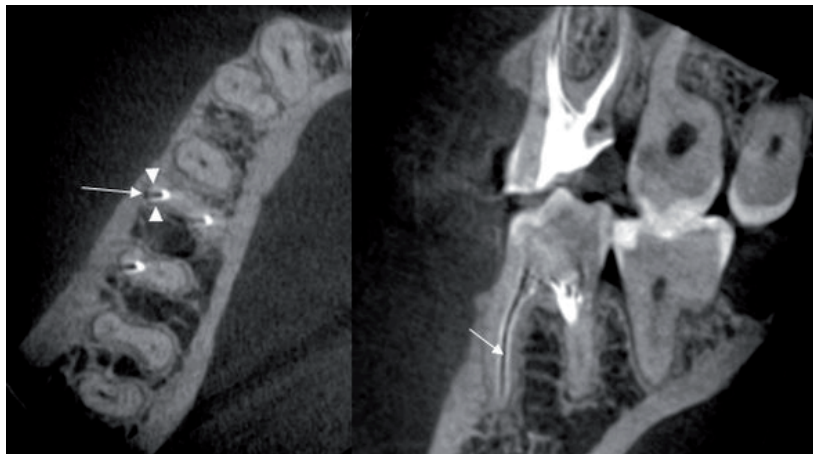


**Figure 3.**  
*The white arrows are showing the dark band caused by the artifact along the root filling of the mesiobuccal root canal of the lower right molar tooth, and the white arrows are pointing to the bright bands on the periphery.*

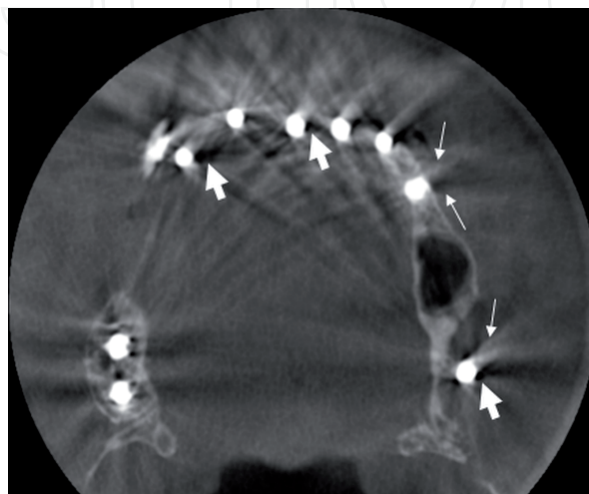


**Figure 4.**  
*The thin white arrows are pointing to bright and dark bands caused by beam hardening, while the thick white arrows are pointing to the transparent areas of missing value artifact.*

in the patient's position lead to error in the reconstruction algorithm, and the reconstructed images show double contour or blurred image [17], as it is presented on a sagittal slice of our CBCT data (**Figure 5**). Spin-Neto et al. reported that the incidence of artifact is higher in CBCT examination of patients under 15 years of age and in small FOV use [18]. Additionally, the patient's displacement of more than 3 mm already causes a significant deterioration of the image quality during exposure [19].

The ring artifact can be described as concentric dark circles on the reconstructed image, mostly on the axial slices (**Figure 6**), indicating the lack of calibration of the detector.

Another possible artifact related to the properties of the CBCT appliance is the aliasing artifact. There are two factors behind: one is the lower frequency of sampling [8], and the other is the geometry of diverging rays emitted from the X-ray tube. This appears on the reconstructed images as lines pointing outward from the

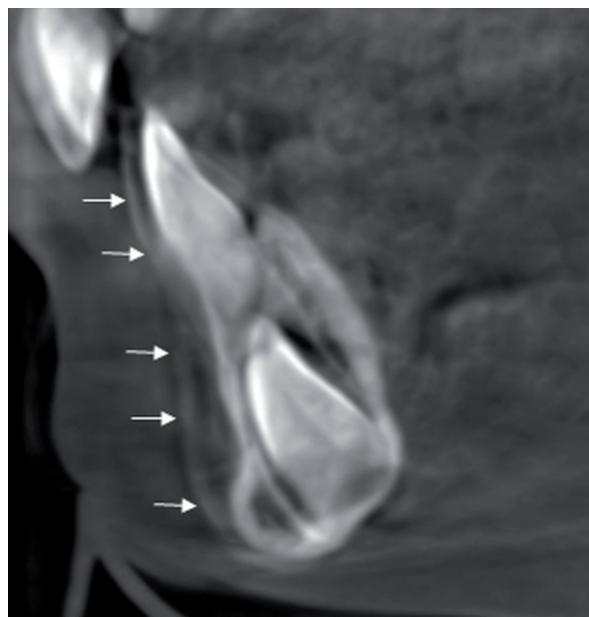


**Figure 5.**  
*Motion artifact on a CBCT scan of a 4-year-old patient in the sagittal plane. The white arrows are pointing to the double contour of the blurred image.*

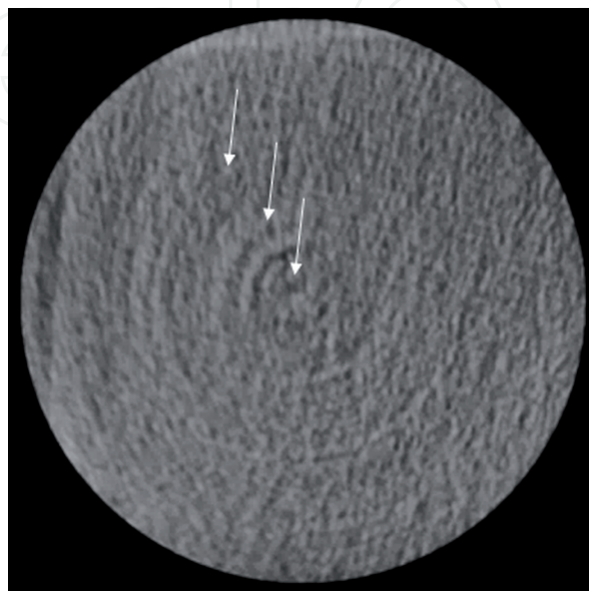


**Figure 6.**  
*The white arrows are pointing to the concentric dark circles.*

center of the image (Moiré pattern) [14] (**Figure 7**). The artifact can usually be compensated by increasing the number of projections and by the built-in image enhancement algorithms [8, 16].

The essence of the partial volume effect is that if there is a larger difference in the density values (e.g., between the dentin and the root canal) at the edge of the imaged object and this area is close to the boundary of two neighboring voxels, the reconstruction algorithm will only calculate an average grayscale value in relation to the entire voxel (**Figure 8**).

Hence, the algorithm calculates a lower value instead of the real density of the object's boundary [20], so a lower grayscale value appears in this peripheral voxel on the reconstructed image, which might lead to an overestimation of the volume [21].



**Figure 7.**

*The white arrows are pointing to the lines appearing farther from the center of the image.*

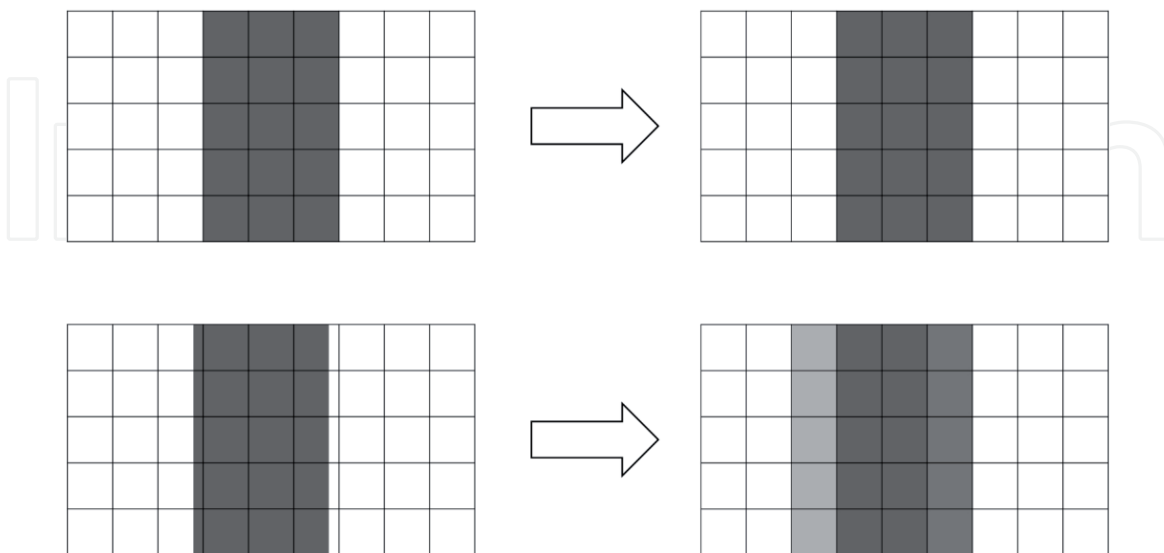


**Figure 8.**

*In the top row, the  $3 \times 5$  pixels in size object “projected” just on the reconstructed pixels, so the real gray scale values of the object are displayed on the reconstructed image. On the bottom row, the object is also  $3 \times 5$  pixels in size but is not “projected” on the reconstructed pixels, so not the actual grayscale values are displayed on the reconstructed image.*

## 4. Imaging of the dentoalveolar region

Since the invention of the CBCT device, numerous publications are concerning the opportunities of CBCT modality in the dentoalveolar region, particularly in endodontics [22–24] and interventions of dentoalveolar surgery [25, 26] as well as orthodontic examinations [27–29]. However, it is important to emphasize that poor image quality can also lead to misdiagnosis and unnecessary exposure to the patient; hence, it is required selecting the appropriate exposure parameters (e.g., FOV, tube voltage, tube current, etc.).

### 4.1 Dentoalveolar surgery

The basis of the proper diagnosis and successful surgical therapy of a pathological disorder is the comprehensive clinical and radiological knowledge of the anatomical region (**Figure 9**). In cases when panoramic radiographs do not provide sufficient information because of the superimpositions of the anatomical landmarks in the assessed regions, CBCT as a three-dimensional modality shall be considered during the justification. The possible indications of CBCT requirement in this field is well known, such as tooth impaction, pre-implant planning, and surgical guide for implant placement. The proper optimization is essential prior to the exposure including the proper selection of the resolution. The latter shall be applicable at a voxel size of 200  $\mu\text{m}$  for linear measurements, though the accuracy is strongly dependent on other parameters of the used CBCT device [30] and the possible smallest FOV shall be set according to the actual clinical situation [31].

### 4.2 Endodontics

Dentists should be aware of the root canal system before the endodontic treatment. Currently, commercially available “high-resolution” CBCTs have a nominal voxel size of 100  $\mu\text{m}$  or even 75  $\mu\text{m}$ , which is comparable in size to the apical constriction of a root canal. CBCT as a modality might be a potential choice in selected cases such as complicated root canal systems, when two-dimensional X-ray technique provides limited information [31] (**Figure 10**).

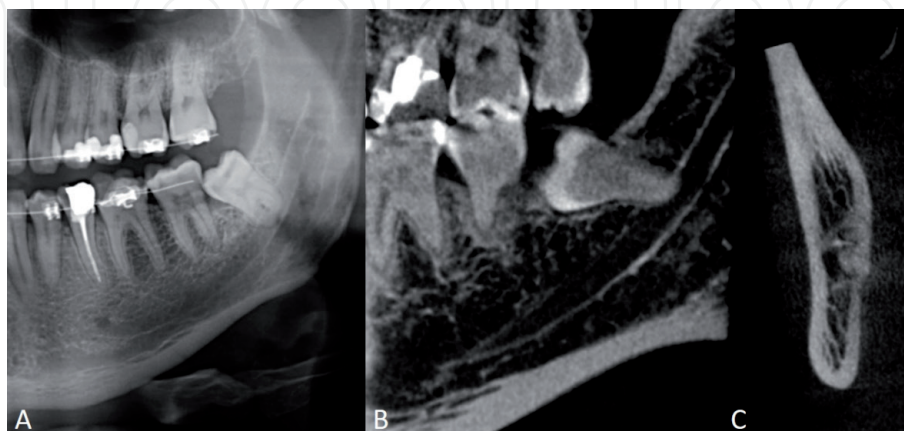


**Figure 9.**

*The relationship of the impacted left lower third molar and left mandibular canal. On the panoramic image, a superimposition is visible (A); however, on the sagittal (B) and coronal (C), CBCT slices the relationship of the apex and the canal is clearly detectable.*

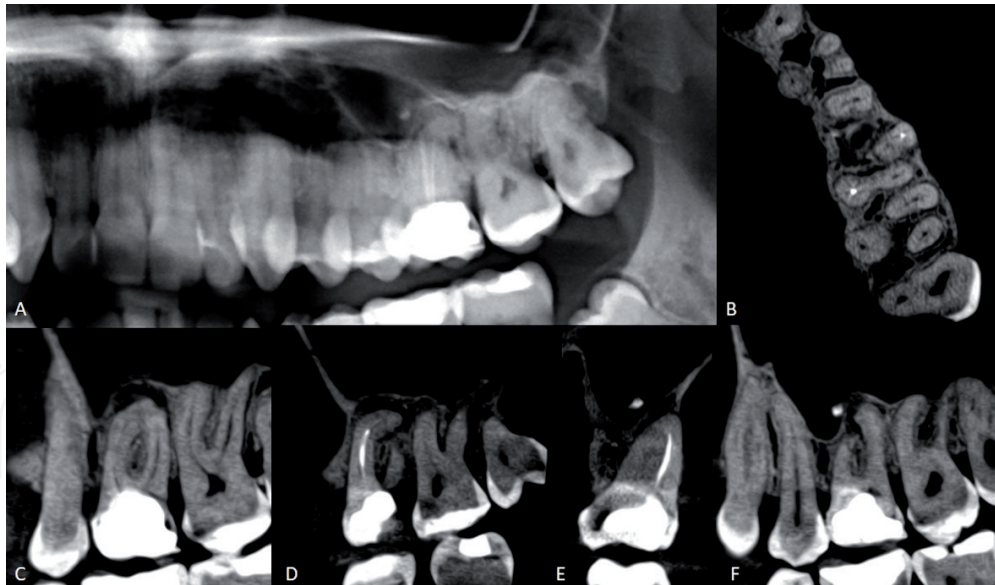


**Figure 10.**

*Insufficient root canal filling of the left upper first molar on the panoramic radiograph (A). The lack of root canal filling of the second mesiobuccal and the distobuccal root canals (B and C). Nearly 90° curvature of the mesiobuccal root and insufficient root canal filling in the first mesiobuccal root canal (D). Hyperdense area in the maxillary sinus potentially due to the extensive use of sealer (E and F). The left upper first premolar is three rooted (B and F).*

### 4.3 Orthodontics

In this field, it is noteworthy to emphasize that the majority of patients are children and young adults [28] who are more sensitive to ionizing radiation. Practitioners must specifically pay attention to the proper justification and optimization during the orthodontic examinations knowing the fact that CBCT as a modality cannot be used routinely [27].

## 5. Imaging of anatomical regions apart from the oral cavity

The appearance of CBCT devices has opened new ways of diagnostic radiology not only in the dentistry but also in the field of facial reconstructive surgery, ENT, rheumatology, and orthopedics. Thanks to the lower radiation dose and the accurate imaging of the bony structures, in many cases, CBCT machines mean a proper diagnostic tool for head and neck radiology [2], especially if we consider the high sensitivity of the eye lens.

### 5.1 CBCT imaging of the paranasal sinuses

All ENT cases make the paranasal sinuses relevant to the anatomical region. One of the most important parameters is the field of view by the CBCT examination of the paranasal sinuses, which should be large enough to include all the sinuses from the frontal sinus to the maxillary sinus (**Figure 11**). Another important rule for the patient's correct position is that the volume should include upper teeth radices to exclude odontogenic sinusitis, which is about 10–12% of all maxillary sinusitis [32].

The frontal and sphenoid sinus, ethmoid cells, maxillary sinuses, and nasal cavity can be studied on the CBCT scan with large field of view. **Figure 1** shows the main anatomical structures of the paranasal sinuses and nasal cavity on CBCT scans.

Although the CBCT imaging has low soft tissue contrast, this method is suitable to detect various signs of inflammation in the paranasal sinuses [33], such as

circulated mucosal thickening, air-fluid level, or polypoid lesions, which typically cause widening in the ostiomeatal complex. Furthermore, thanks to visualization of the radices, we can differ the odontogenic and nonodontogenic sinusitis (**Figure 12**). By the malignant lesion, the most important radiological mark is the bone destruction, and in this case, additional imaging techniques, for example, contrast enhanced magnetic resonance imaging (MRI) or CT, are necessary for the accurate diagnosis.

## 5.2 CBCT imaging of the ear

Nowadays much more CBCT devices are suitable for the examination of the external, middle, and inner ear structures based on high-spatial resolution. For the valuable imaging of the ears, small FOV, low voxel size, approximately 100  $\mu\text{m}$ , and precise patient positioning are required. It is possible to create scan one side or both sides during one rotation, and normally, the whole ear from the skull base to the mastoid process is in the volume tomogram. One of the main advantages of this technique is the low radiation dose opposite to the high-resolution CT, which is an alternative radiologic method to analyze the middle ear ossicles. In the literature, there are some articles that compare reliability of the two techniques for the detection of otosclerosis, but there is no consensus in this question [34–37].

On the CBCT scan, we can identify the external auditory canal, the tympanic cavity with the ossicles [38], and the inner ear structures such as cochlea, semicircular canals, and the facial nerve (**Figure 13**). For the accurate diagnosis, different reconstructions are useful, such as Pöschl reformat for the evaluation of SSC and

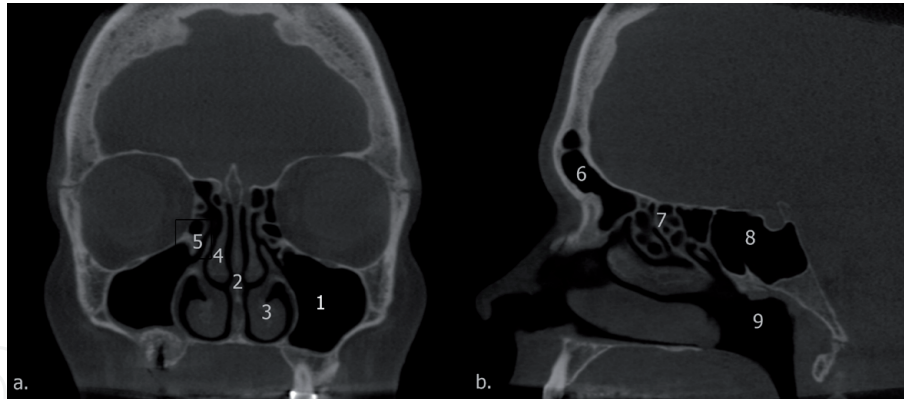


**Figure 11.** The main anatomical structures of the paranasal sinuses in coronal (a) and sagittal (b) view (1: maxillary sinus, 2: nasal septum, 3: inferior nasal concha, 4: middle nasal concha, 5: ostiomeatal complex, 6: frontal sinus, 7: ethmoid cells, 8: sphenoid sinus, 9: nasopharynx).



**Figure 12.** Sinusitis with oroantral fistula on CBCT scan.

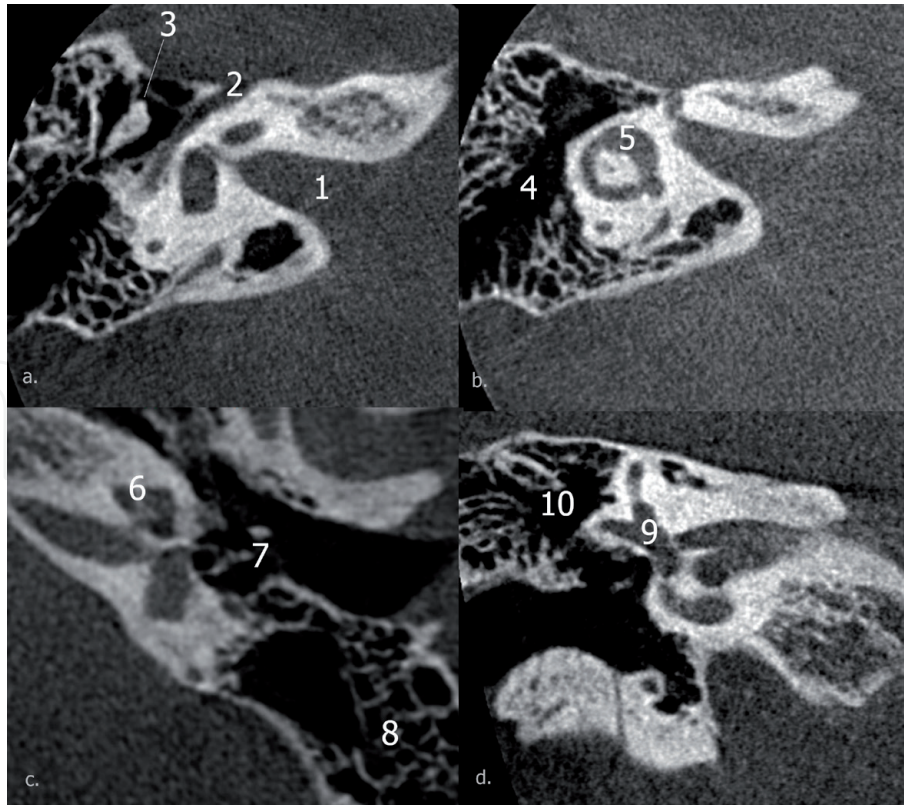


**Figure 13.** External, middle, and inner ear structures on CBCT scans (1: internal auditory canal, 2: facial nerve, 3: malleus and incus, 4: tympanic cavity, 5: vestibule and lateral semicircular canal, 6: cochlea, 7: stapes, 8: mastoid cells, 9: semicircular canals, 10: epitympanum).

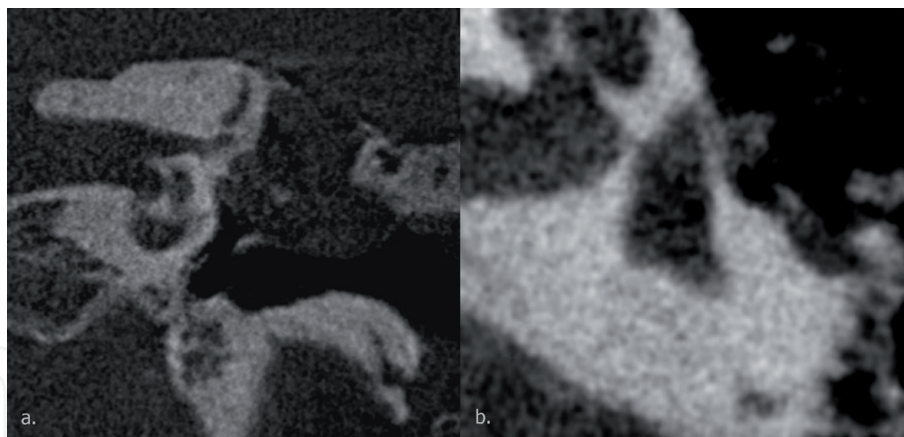


**Figure 14.** The image “a” shows cholesteatoma with bone destruction on the tympanic tegmen, and image “b” shows otosclerosis of the stapes.

vestibular aqueduct or Stenvers reformat for the assessment of cochlea, facial nerve, and round window [39].

On the CBCT data, the radiologist can exclude lesions in the external auditory canal, in the tympanic cavity, or in the antromastoidal parts. The most frequently, inflammation can be found in the middle ear cavity or in the mastoid, but special lesions, for instance, glomus tympanicum or cholesteatoma, can be also detected on CBCT images. Despite the poor soft tissue contrast on the CBCT image sequences, there are radiological signs that are characteristic of the above-mentioned lesions. For example, bone destruction and location in the Prussak space are characteristic for the cholesteatoma, and the location on the cochlear promontory is typical for a glomus tympanicum paraganglioma (Figure 14).

### **5.3 CBCT imaging of maxillofacial bones**

CBCT imaging is one of the best options for the diagnosis of facial bones, as it can accurately visualize the bone structures and reduce the metal artifact, e.g., from dental implants and crowns, more than conventional CT [40]. The evaluation of the whole facial skull is relevant in the field of the orthognathic and reconstructive surgery; therefore, large field of view is necessary but because of the minimalization of radiation dose larger, e.g., 0.3–0.4 mm voxel size is enough for the correct diagnosis. The CBCT imaging is suitable to detect facial fractures, craniofacial anomalies, bone tumor, or osteomyelitis. Besides of the diagnostics, frequently other aim of this examination is the preoperative surgical planning for orthognathic operation [41], which needs special 3D cephalometric software.

### **5.4 CBCT imaging of the airway**

The CBCT volumetric data with large FOV can be used for the assessment of the upper airways [42, 43]. The volumetric measurement of the airways can facilitate the diagnosis of the patient with obstructive sleep apnea, and it can play an important role in the planning of orthodontic treatment [44, 45].

### **5.5 CBCT imaging of joints**

Most of the CBCT devices are small size devices compared to the conventional CT, by which the patient stands or sits during the exposition. On the market, there are only a few CBCT appliances available in which the patient lies, and the device can scan the joints of the upper and lower extremity and the whole spine. Several constructions of CBCT machines are capable specifically for the joints of upper and lower extremity. These techniques provide the diagnosis of degenerative joint disease, arthritis, tumor-like bone lesion, and fracture of the bones [46, 47].

## **6. Incidental findings on CBCT image sequences**

Frequently in the field of dentistry and ENT large volume, CBCT scans are required for the diagnosis and treatment planning. The increasing of the volume increases the frequency of the incidental findings. Many articles examined the distribution of incidental findings in the dentomaxillofacial CBCT dataset, and the most common incidental findings are the intracranial calcification, frontal hyperostosis, tonsillolith, styloid calcification, antrolith, and artery calcification [48].

### **6.1 Intracranial calcification**

The large volume dental or ENT volume tomogram involves intracranial anatomical structures. One of the most frequent incidental findings is the calcification of the internal carotid artery, in which typical location is by the carotid syphons. The other typical place of the calcification is along the superior sagittal sinus by the cerebral falx.

### **6.2 Tonsillolith**

On the CBCT images, the small calcifications as hyperdense foci are easy to detect; therefore, this imaging technique is capable to visualize small tonsilloliths (**Figure 15**). These calcification clusters can be in or around the tonsils.

These calculi cause no symptoms, and usually, these are only incidental findings, but other pathologies, e.g., foreign bodies, should be distinguished from these stones.

### 6.3 Styloid calcification

The calcification of the styloid ligament or the elongated styloid process is also known as Eagle syndrome (**Figure 16**), which is usually an incidental finding, but it can cause various symptoms, such as restricted mouth opening, shooting pain in the mandible, pressure in the throat, difficult swallowing, or by the compression on the internal carotid artery or internal jugular vein, and it can lead to intracranial pressure and transient ischemic attack.

### 6.4 Antrolith

Antroliths are calcifications within the maxillary sinus, which are mostly asymptomatic, and require no treatment (**Figure 17**). On the other hand, larger antroliths may be a symptom of chronic sinusitis or fungal sinusitis, which may involve surgical removal. Antroliths are hyperdense foci or larger masses that are often embedded in the mucoperiosteum in the CBCT images.

### 6.5 Artery calcification

One of the most frequent incidental findings on CBCT scans is the calcification of the carotid arteries. The calcifications are hyperdensity along the vessels. As the

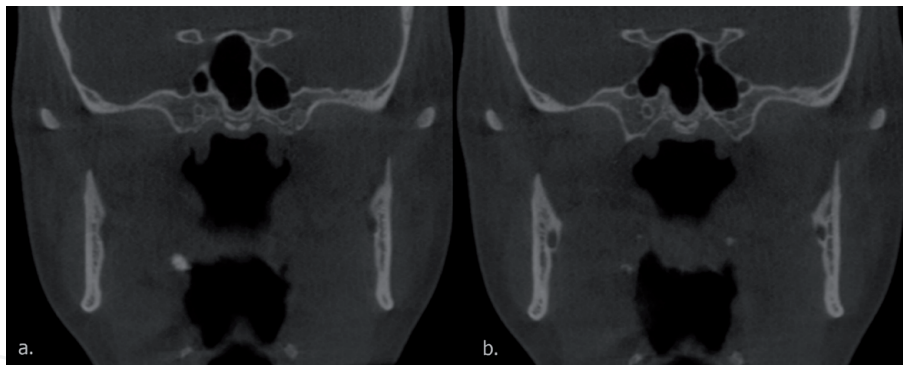


**Figure 15.**  
*Tonsillolith as hyperintense foci by the tonsils (a and b).*



**Figure 16.**  
*Calcification of the styloid ligament.*



**Figure 17.**  
*Calcification in the right maxillary sinus with mucosal thickening.*

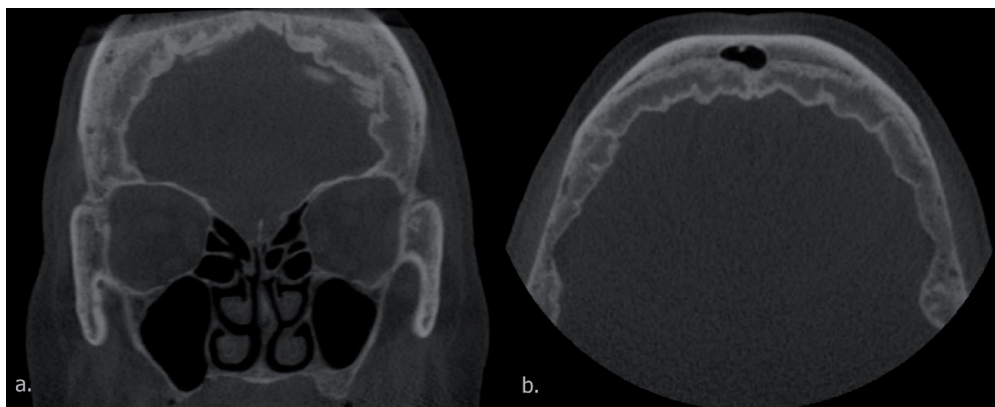


**Figure 18.**  
*Hyperostosis frontalis in coronal (a) and axial (b) view.*

outcome of the calcification of the internal carotid artery can be stroke, the following stenosis with ultrasound is important.

### 6.6 Hyperostosis frontalis interna

Hyperostosis frontalis interna is a benign bone formation on the inner table of the frontal bone (**Figure 18**). Normally, it is a symmetric bone thickening, and sometimes, it involves the parietal bones also. The relevance of this disorder is in the differential diagnosis and to distinguish from the pathology such as sclerotic metastases, Paget disease, or fibrous dysplasia.

## 7. Limitations and expected improvements

One limitation of the present CBCT technology is the high dependence of resolution to the object diameter. This is the reason why this technology is used on head and neck or extremity imaging. The diameter of the chest and abdomen is too big to get higher resolution images than MSCT. Another disadvantage of CBCT is its low quality in soft tissue imaging. Relatively low radiation dose combined with short exposure time provides low quality images of soft tissue structures. This is another reason for CBCT not to use chest and abdomen imaging.

CBCT technology is highly sensitive to object's movement because of the high resolution and of the low number of projection images used for reconstruction.

Usually, it is a challenge to control movements of patient, especially during head imaging. Some positions of the body lower head movements like supine position. Patient movement correction algorithms are available. X-ray scanning combined with video recording the actual movements of patient can be a useful method. Software can analyze and compensate for slight movements gained from video control and provides improved quality images [18].

Filtered back projection based on FDK algorithm is widely used way of reconstruction for CBCT technology. This reconstruction used in wide energy spectrum of X-ray beam arises some artifacts like beam hardening resulting in increased noise of images and misdiagnosis in clinical practice. Beam hardening reduction software is commonly used to improve images; however, this works as an image filtering. In one of our previous study, Monte Carlo analysis was used to compare beam hardening software in reducing beam hardening artifact errors and error by synchrotron micro-CT. Results showed that the beam hardening artifact reduction was comparable with synchrotron micro-CT images [49].

Along with beam hardening artifact scatters (metal artifacts) around the high density metal, implant material frequently causes clinical diagnostic problems since observers unable to detect bone tissue surrounding the implant surface [9]. Soft tissue contrast is further influenced by scatter [50]. Manufacturers usually provide post-processing metal artifact reduction software. Unfortunately this image enhancement is a filter method resulting in loss of peri-implant bone tissue on images [51]. In contrast to maximum likelihood expectation, maximization iterative reconstruction algorithms have proved to improve image quality and to increase signal-to-noise ratio [52]. At present, this is not a widely used method because of the limited capacity of personal computers. However, this way of reconstruction is able to provide image on peri-implant bone tissue. Another way for significant reduction of scatter is dual-energy imaging technology. In a study where single-energy CBCT and dual-energy CBCT were compared, metal artifact with the use of upstream filter on dual energy CT was significantly reduced. This method also resulted in higher signal-to-noise values [53].

Photon-counting CT is a state-of-art technology with the potential to dramatically change clinical 3D imaging. The hybrid-pixel photon-counting detector concept was first demonstrated at CERN in 1991 [54]. The detection of X-ray photons is realized by discriminators, which register a photon only if its energy exceeds a certain threshold value. This way the electronic noise is effectively eliminated and the detector does not affected by dark current signals. Implementation of additional discriminators with different threshold levels to the detector results in discrimination of polychromatic X-ray spectrum into several distinct energy bins [55].

Photon-counting CBCTs are able to reduce radiation dose, reconstruct images at a higher resolution, rectify beam-hardening artifacts, optimize contrast agents' use, and create opportunities for quantitative imaging relative to current CBCT technology [56].

## **Conflict of interest**

The authors declare no conflict of interest.

IntechOpen

### Author details

Bence Tamás Szabó<sup>1\*</sup>, Adrienn Dobai<sup>1,2</sup> and Csaba Dobo-Nagy<sup>1</sup>

1 Department of Oral Diagnostics, Faculty of Dentistry, Semmelweis University, Budapest, Hungary

2 Department of Oral Diagnostics, Faculty of Dentistry and Magnetic Resonance Research Center, Faculty of Medicine, Semmelweis University, Budapest, Hungary

\*Address all correspondence to: [szabo.bence\\_tamas@dent.semmelweis-univ.hu](mailto:szabo.bence_tamas@dent.semmelweis-univ.hu)

### IntechOpen

© 2020 The Author(s). Licensee IntechOpen. This chapter is distributed under the terms of the Creative Commons Attribution License (<http://creativecommons.org/licenses/by/3.0>), which permits unrestricted use, distribution, and reproduction in any medium, provided the original work is properly cited. 

## References

- [1] Farman AG, Scarfe WC. Historical perspectives on CBCT. In: Scarfe WC, Angelopoulos C, editors. Maxillofacial Cone Beam Computed Tomography. Louisville: Springer; 2018. pp. 3-11. DOI: 10.1007/978-3-319-62061-9
- [2] Al Abduwani J, Zilin Skiene L, Colley S, Ahmed S. Cone beam CT paranasal sinuses versus standard multidetector and low dose multidetector CT studies. American Journal of Otolaryngology. 2016;**37**:59-64. DOI: 10.1016/j.amjoto.2015.08.002
- [3] Brüllmann D, Schulze R. Spatial resolution in CBCT machines for dental/maxillofacial applications-what do we know today? Dentomaxillofacial Radiology. 2015;**44**:20140204. DOI: 10.1259/dmfr.20140204
- [4] Nasseh I, Al-Rawi W. Cone beam computed tomography. Dental Clinics of North America. 2018;**62**:361-391. DOI: 10.1016/j.cden.2018.03.002
- [5] Ludlow JB, Timothy R, Walker C, Hunter R, Benavides E, Samuelson DB, et al. Effective dose of dental CBCT-a meta analysis of published data and additional data for nine CBCT units. Dentomaxillofacial Radiology. 2015;**44**:20140197. DOI: 10.1259/dmfr.20140197
- [6] Pauwels R, Seynaeve L, Henriques JC, de Oliveira-Santos C, Souza PC, Westphalen FH, et al. Optimization of dental CBCT exposures through mAs reduction. Dentomaxillofacial Radiology. 2015;**44**:20150108. DOI: 10.1259/dmfr.20150108
- [7] Pauwels R, Araki K, Siewerdsen JH, Thongvigitmanee SS. Technical aspects of dental CBCT: State of the art Dentomaxillofacial Radiology. 2014;**44**:20140224. DOI: 10.1259/dmfr.20140224
- [8] Pauwels R. What is CBCT and how does it work? In: Scarfe WC, Angelopoulos C, editors. Maxillofacial Cone Beam Computed Tomography. Louisville: Springer; 2018. pp. 13-42. DOI: 10.1007/978-3-319-62061-9
- [9] Kovács M, Fejérdy P, Dobó Nagy CS. A fém műtermék a fejnnyaki cone-beam CT (CBCT) képeken. Fogorvosi Szemle. 2008;**5**:171-178
- [10] Abramovitch K, Rice DD. Basic principles of cone beam computed tomography. Dental Clinics of North America. 2014;**58**:463-484. DOI: 10.1016/j.cden.2014.03.002
- [11] Perényi Á, Bella Z, Baráth Z, Magyar P, Nagy K, Rovó L. A cone-beam komputertomográfia alkalmazása a fül-orr-gégészeti képalkotásban. Orvosi Hetilap. 2016;**157**:52-58. DOI: 10.1556/650.2016.30334
- [12] Nemtoi A, Czink C, Haba D, Gahleitner A. Cone beam CT: A current overview of devices. Dentomaxillofacial Radiology. 2013;**4**:20120443. DOI: 10.1259/dmfr.20120443
- [13] Feldkamp LA, Davis LC, Kress JW. Practical cone-beam algorithm. Journal of the Optical Society of America. A. 1984;**1**:612-619. DOI: 10.1364/JOSAA.1.000612
- [14] Schulze R, Heil U, Grob D, Bruellmann DD, Dranischnikow E, Schwanecke U, et al. Artefacts in CBCT: A review. Dentomaxillofacial Radiology. 2011;**40**:265-273. DOI: 10.1259/dmfr/30642039
- [15] Nagarajappa AK, Dwivedi N, Tiwari R. Artifacts: The downturn of CBCT image. Journal of International Society of Preventive & Community Dentistry. 2015;**5**:440-445. DOI: 10.4103/2231-0762.170523

- [16] Schulze R, Scarfe WC, Molteni R, Mozzo P, Quality I. In: Scarfe WC, Angelopoulos C, editors. *Maxillofacial Cone Beam Computed Tomography*. Louisville: Springer; 2018. pp. 95-112. DOI: 10.1007/978-3-319-62061-9
- [17] Spin-Neto R, Wenzel A. Patient movement and motion artefacts in cone beam computed tomography of the dentomaxillofacial region: A systematic literature review. *Oral Surgery, Oral Medicine, Oral Pathology, Oral Radiology*. 2016;**121**:425-433. DOI: 10.1016/j.oooo.2015.11.019
- [18] Spin-Neto R, Matzen LH, Schropp L, Gotfredsen E, Wenzel A. Factors affecting patient movement and re-exposure in cone beam computed tomography examination. *Oral Surgery, Oral Medicine, Oral Pathology, Oral Radiology*. 2015;**119**:572-578. DOI: 10.1016/j.oooo.2015.01.011
- [19] Spin-Neto R, Costa C, Salgado DM, Zambrana NR, Gotfredsen E, Wenzel A. Patient movement characteristics and the impact on CBCT image quality and interpretability. *Dentomaxillofacial Radiology*. 2018;**47**:20170216. DOI: 10.1259/dmfr.20170216
- [20] Glover GH, Pelc NJ. Nonlinear partial volume artifacts in x-ray computed tomography. *Medical Physics*. 1980;**7**:238-248. DOI: 10.1118/1.594678
- [21] Ye N, Jian F. Effect of voxel size and partial volume effect on accuracy of tooth volumetric measurements with cone beam CT. *Dentomaxillofacial Radiology*. 2013;**42**:20130070. DOI: 10.1259/dmfr.20130070
- [22] Scarfe WC, Levin MD, Gane D, Farman AG. Use of cone beam computed tomography in endodontics. *International Journal of Dentistry*. 2009;**2009**:634567. DOI: 10.1155/2009/634567
- [23] Michetti J, Maret D, Mallet JP, Diemer F. Validation of cone beam computed tomography as a tool to explore root canal anatomy. *Journal of Endodontics*. 2010;**36**:1187-1190. DOI: 10.1016/j.joen.2010.03.029
- [24] Szabo BT, Pataky L, Mikusi R, Fejerdy P, Dobo-Nagy C. Comparative evaluation of cone-beam CT equipment with micro-CT in the visualization of root canal system. *Annali dell'Istituto Superiore di Sanità*. 2012;**48**:49-52. DOI: 10.4415/ANN\_12\_01\_08
- [25] Van Dessel J, Nicolielo LFP, Huang Y, Coudyzer W, Salmon B, Lambrichts I, et al. Accuracy and reliability of different cone beam computed tomography (CBCT) devices for structural analysis of alveolar bone in comparison with multislice CT and micro-CT. *European Journal of Oral Implantology*. 2017;**10**:95-105
- [26] Parsa A, Ibrahim N, Hassan B, van der Stelt P, Wismeijer D. Bone quality evaluation at dental implant site using multislice CT, micro-CT, and cone beam CT. *Clinical Oral Implants Research*. 2015;**26**:e1-e7. DOI: 10.1111/clr.12315
- [27] De Grauwe A, Ayaz I, Shujaat S, Dimitrov S, Gbadegbegnon L, Vande Vannet B, et al. CBCT in orthodontics: A systematic review on justification of CBCT in a paediatric population prior to orthodontic treatment. *European Journal of Orthodontics*. 2019;**41**:381-389. DOI: 10.1093/ejo/cjy066
- [28] Kapila SD, Nervina JM. CBCT in orthodontics: Assessment of treatment outcomes and indications for its use. *Dentomaxillofacial Radiology*. 2014;**44**:20140282. DOI: 10.1259/dmfr.20140282
- [29] Dobai A, Vizkelety T, Markella Z, Rosta A, Kucserá Á, Barabás J. Az alsó archarmad Di Paolo-féle vizsgálatá Cone-Beam CT adatállományon. *Fogorvosi Szemle*. 2016;**109**:39-44

- [30] Jacobs R, Salmon B, Codari M, Hassan B, Bornstein MM. Cone beam computed tomography in implant dentistry: Recommendations for clinical use. *BMC Oral Health*. 2018;**18**:88. DOI: 10.1186/s12903-018-0523-5
- [31] SEDENTEXCT Guideline Development Panel. Radiation Protection No 172. Cone Beam CT for Dental and Maxillofacial Radiology. Evidence Based Guidelines [Internet]. 2012. Available from: [http://www.sedentexct.eu/files/radiation\\_protection\\_172.pdf](http://www.sedentexct.eu/files/radiation_protection_172.pdf) [Accessed: 13 December 2019]
- [32] Mehra P, Jeong D. Maxillary sinusitis of odontogenic origin. *Current Infectious Disease Reports*. 2008;**10**:205-210. DOI: 10.1007/s11908-008-0034-7
- [33] Stutzki M, Jahns E, Mandapathil MM, Diogo I, Werner JA, Guldner C. Indications of cone beam CT in head and neck imaging. *Acta Oto-Laryngologica*. 2015;**135**:1337-1343. DOI: 10.3109/00016489.2015.1076172
- [34] Nardi C, Talamonti C, Pallotta S, Saletti P, Calistri L, Cordopatri C, et al. Head and neck effective dose and quantitative assessment of image quality: A study to compare cone beam CT and multislice spiral CT. *Dentomaxillofacial Radiology*. 2017;**46**:20170030. DOI: 10.1259/dmfr.20170030
- [35] Razafindranaly V, Truy E, Pialat JB, Martinon A, Bourhis M, Boublay N, et al. Cone beam CT versus multislice CT: Radiologic diagnostic agreement in the postoperative assessment of cochlear implantation. *Otology & Neurotology*. 2016;**37**:1246-1254. DOI: 10.1097/mao.0000000000001165
- [36] Dahmani-Causse M, Marx M, Deguine O, Fraysse B, Lepage B, Escude B. Morphologic examination of the temporal bone by cone beam computed tomography: Comparison with multislice helical computed tomography. *European Annals of Otorhinolaryngology, Head and Neck Diseases*. 2011;**128**:230-235. DOI: 10.1016/j.anorl.2011.02.016
- [37] Revesz P, Liktor B, Liktor B, Sziklai I, Gerlinger I, Karosi T. Comparative analysis of preoperative diagnostic values of HRCT and CBCT in patients with histologically diagnosed otosclerotic stapes footplates. *European Archives of Oto-Rhino-Laryngology*. 2016;**273**:63-72. DOI: 10.1007/s00405-015-3490-3
- [38] Guldner C, Diogo I, Bernd E, Drager S, Mandapathil M, Teymoortash A, et al. Visualization of anatomy in normal and pathologic middle ears by cone beam CT. *European Archives of Oto-Rhino-Laryngology*. 2017;**274**:737-742. DOI: 10.1007/s00405-016-4345-2
- [39] Reformation in CT of the Temporal Bone [Internet]. 2016. Available from: <https://radiologykey.com/reformation-in-ct-of-the-temporal-bone> [Accessed: 13 December 2019]
- [40] Shintaku WH, Venturin JS, Azevedo B, Noujeim M. Applications of cone-beam computed tomography in fractures of the maxillofacial complex. *Dental Traumatology*. 2009;**25**:358-366. DOI: 10.1111/j.1600-9657.2009.00795.x
- [41] Bai L, Li L, Su K, Bleyer A, Zhang Y, Ji P. 3D reconstruction images of cone beam computed tomography applied to maxillofacial fractures: A case study and mini review. *Journal of X-Ray Science and Technology*. 2018;**26**:115-123. DOI: 10.3233/xst-17342
- [42] Zimmerman JN, Lee J, Pliska BT. Reliability of upper pharyngeal airway assessment using dental CBCT: A systematic review. *European Journal of Orthodontics*. 2017;**39**(5):489-496. DOI: 10.1093/ejo/cjw079

- [43] Souza KR, Oltramari-Navarro PV, Navarro Rde L, Conti AC, Almeida MR. Reliability of a method to conduct upper airway analysis in cone-beam computed tomography. *Brazilian Oral Research*. 2013;**27**:48-54. DOI: 10.1590/s1806-83242013000100009
- [44] Chen H, Li Y, Reiber JH, de Lange J, Tu S, van der Stelt P, et al. Analyses of aerodynamic characteristics of the oropharynx applying CBCT: Obstructive sleep apnea patients versus control subjects. *Dentomaxillofacial Radiology*. 2018;**47**:20170238. DOI: 10.1259/dmfr.20170238
- [45] Obelenis Ryan DP, Bianchi J, Ignacio J, Wolford LM, Goncalves JR. Cone-beam computed tomography airway measurements: Can we trust them? *American Journal of Orthodontics and Dentofacial Orthopedics*. 2019;**156**:53-60. DOI: 10.1016/j.ajodo.2018.07.024
- [46] Jaroma A, Suomalainen JS, Niemitukia L, Soininvaara T, Salo J, Kroger H. Imaging of symptomatic total knee arthroplasty with cone beam computed tomography. *Acta Radiologica*. 2018;**59**(12):1500-1507. DOI: 10.1177/0284185118762247
- [47] Pallaver A, Honigmann P. The role of cone-beam computed tomography (CBCT) scan for detection and follow-up of traumatic wrist pathologies. *The Journal of Hand Surgery*. 2019;**44**:1081-1087. DOI: 10.1016/j.jhssa.2019.07.014
- [48] Barghan S, Tahmasbi Arashlow M, Nair MK. Incidental findings on cone beam computed tomography studies outside of the maxillofacial skeleton. *International Journal of Dentistry*. 2016;**2016**:9196503. DOI: 10.1155/2016/9196503
- [49] Kovács M, Danyi R, Erdélyi M, Fejérdy P, Dobo-Nagy C. Distortional effect of beam-hardening artefacts on microCT: A simulation study based on an in vitro caries model. *Oral Surgery, Oral Medicine, Oral Pathology, Oral Radiology, and Endodontics*. 2009;**108**:591-599. DOI: 10.1016/j.tripleo.2009.06.009
- [50] Tofts PS, Gore JC. Some sources of artefact in computed tomography. *Physics in Medicine and Biology*. 1980;**25**:117-127
- [51] Ferreira JB, Christovam IO, Alencar DS, da Motta AFJ, Mattos CT, Cury-Saramago A. Accuracy and reproducibility of dental measurements on tomographic digital models: A systematic review and meta-analysis. *Dentomaxillofacial Radiology*. 2017;**46**:20160455. DOI: 10.1259/dmfr.20160455
- [52] Bechara BB, Moore WS, McMahan CA, Noujeim M. Metal artefact reduction with cone beam CT: An in vitro study. *Dentomaxillofacial Radiology*. 2012;**41**:248-253. DOI: 10.1259/dmfr/80899839
- [53] Iramina H, Hamaguchi T, Nakamura M, Mizowaki T, Kanno I. Metal artifact reduction by filter-based dual-energy cone-beam computed tomography on a bench-top micro-CBCT system: Concept and demonstration. *Journal of Radiation Research*. 2018;**59**:511-520. DOI: 10.1093/jrr/rry034
- [54] Anghinolfi F, Aspell P, Bass K, Beusch W, Bosisio L, Boutonnet C, et al. A 1006 element hybrid silicon pixel detector with strobed binary output. *IEEE Transactions on Nuclear Science*. 1992;**39**:654-661. DOI: 10.1109/23.159682
- [55] Sellerer T, Ehn S, Mechlem K, Duda M, Epple M, Noe PB, et al. Quantitative dual-energy micro-CT with a photon-counting detector for material science and non-destructive testing.

PLoS One. 2019;**14**:e0219659. DOI:  
10.1371/journal.pone.0219659

[56] Willemink JM, Pourmorteza A,  
Pelc JN, Fleischmann D. Photon-  
counting CT: Technical principles  
and clinical prospects. *Radiology*.  
2018;**289**:293-312. DOI: 10.1148/  
radiol.2018172656

IntechOpen

IntechOpen